

# Wideband Circularly Polarized Planar Antenna for X-Band Applications

May Abo El-Hassan\*, Asmaa E. Farahat, and Khalid F. A. Hussein

**Abstract**—A wide band circularly polarized planar antenna of high radiation efficiency is proposed in the present work for future generations of wireless communications requiring circular polarization in the X-band of the microwave spectrum. The main radiating part of the antenna is a rectangular turn-shaped strip that is capacitively loaded by two corner-shaped parasitic elements. The antenna is fed through coplanar waveguide (CPW) region whose ground structure is defected by etching two rectangular annular slots. The purposes of both the corner-shaped parasitic elements and the rectangular annular slots of the CPW ground plane are to increase the impedance matching and 3 dB axial ratio (AR) bandwidth, and to enhance the antenna efficiency. The design is achieved through complete parametric study to find the optimum dimensions of the antenna. A prototype of the proposed antenna is fabricated for the experimental assessment of its performance. The results obtained by both simulation and experimental measurements show that the impedance matching bandwidth is about 5.3 GHz (8–13.3 GHz); the 3 dB AR bandwidth is about 3.1 GHz (8–11.1 GHz); the maximum gain ranges from 4.5 to 5.5 dBi; and the radiation efficiency is higher than 98% over the operational frequency band.

## 1. INTRODUCTION

Circular polarization is a vital requirement in many applications such as satellite communications, radar systems, mobile communications, and wireless sensor networks [1]. Moreover, wideband compact size circularly polarized (CP) antenna is recommended to overcome the many problems such as Faraday rotation and orientation mismatch between the transmitting and receiving antennas [2]. The main drawback of the microstrip patch antennas when they are designed to produce circular polarization is limited 3 dB axial ratio (AR) bandwidth. In the recent literature, several techniques have been proposed to achieve wide-band antenna designs rather than the conventional microstrip patch antennas. In [2], broadband impedance matching and wide 3 dB-AR bandwidth are obtained by a monopole antenna with parasitic strips and dualstub loading. In [3], a slot antenna fed through a coplanar waveguide (CPW) with defected ground plane is proposed to produce dual-band circular polarization. In [4], an I-shaped slot antenna fed through a CPW is proposed to produce broadband circular polarization for C-band and X-band applications. The work of [5] proposes a CP antenna composed of a square aperture in the ground plane with parasitic patches to enhance the impedance matching bandwidth. Also, many other research efforts and trials have been presented in some recent publications which arrive at CP antennas with wide frequency band for impedance matching and 3 dB AR [6–12].

The present work proposes a planar antenna composed of a rectangular turn-shaped strip that is capacitively loaded by two corner-shaped parasitic strips. The antenna is fed through CPW region whose ground structure is defected by etching two rectangular annular slots. The purposes of both the corner-shaped parasitic elements and the rectangular annular slots of the CPW ground plane are to increase the bandwidth of impedance matching and 3 dB AR, and to enhance the antenna efficiency.

---

*Received 24 July 2023, Accepted 1 September 2023, Scheduled 17 September 2023*

\* Corresponding author: May Abo El-Hassan (mayaboelhassan@yahoo.com).

The authors are with the Microwave Engineering Department, Electronics Research Institute (ERI) Cairo, Egypt.

The present paper is organized in six sections following the introduction. Section 2 presents the proposed antenna design. Section 3 describes the fabrication of the antenna prototype and the measurement of the reflection coefficient. Section 4 presents the radiation patterns produced by the antenna. Section 5 presents the antenna gain and radiation efficiency. Section 6 provides interesting comparisons with other designs available in some recent literature. Finally, Section 7 presents the most important conclusions of the present paper.

## 2. ANTENNA DESIGN

The detailed design of the wideband CP antenna proposed in the present work is explained.

### 2.1. Antenna Geometry

The proposed antenna geometry is presented in Figure 1. This antenna can be viewed as a rectangular turn-like wide strip fed through a CPW region whose dimensions are set to realize impedance matching over a wide frequency band.

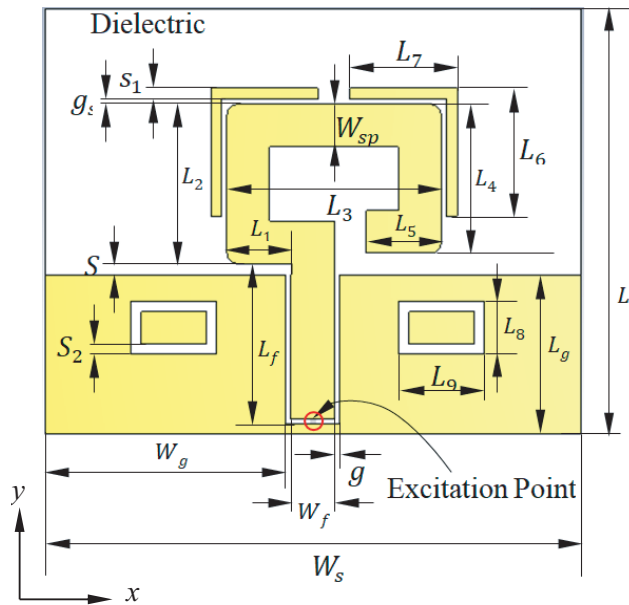


**Figure 1.** Geometry of the proposed circularly polarized printed antenna showing the optimum dimensions.

As shown in Figure 1, the CPW region has defects in the two-sided ground structure. The turn-shaped strip is the radiating element and can be considered as an extension of the central strip of the CPW. For improving the antenna performance regarding the circular polarization and the operational bandwidth the radiating strip is capacitively loaded by corner-shaped narrow strips as shown in Figure 1. Also, the defects of the side ground regions of the CPW take the form of rectangular ring aperture whose role is to increase the 3 dB-AR bandwidth. The dimensional parameters of turn-like strip radiator, corner-shaped narrow strip parasitic elements, CPW region, and rectangular aperture in the side grounds are presented in Figure 1. As shown in Figure 1, the overall antenna dimension is  $L_s \times W_s$ , and it is fabricated on a Rogers RO3003 substrate of height  $h = 0.13$  mm, dielectric constant  $\epsilon_r = 3$ , and loss tangent  $\tan \delta = 0.001$ . The designed antenna is constructed by a turn-shaped strip radiating patch which is chosen to resonate over the frequency band 8–13.3 GHz. Thus, the bandwidth is 5.3 GHz. The dimensions of turn-shaped strip patch antenna are:  $L_1, L_2, L_3, L_4, L_5$ , and the turn-shaped strip width is  $W_{sp}$  which is connected to coplanar waveguide feedline, having length and width of  $L_f \times W_f$  and gap  $g$  of distance designed for a  $50 \Omega$  characteristic impedance. The length and width of the ground plane are  $L_g \times W_g$ . The spacing between edge of the ground plane and turn-shaped strip is  $S$ .

The total efficiency,  $\eta$ , of the proposed antenna can be expressed as follows.

$$\eta = \eta_{rad} (1 - |S_{11}|^2) \tag{1}$$

where  $\eta_{rad}$  is the radiation efficiency, and  $S_{11}$  is the reflection coefficient at the antenna feeding port.

The radiation efficiency can be expressed as follows.

$$\eta_{rad} = 1 - L \tag{2}$$

where  $L$  is the total losses of the antenna other than the return loss.

In addition to the conductor and dielectric losses of the antenna material, a circularly polarized antenna has additional polarization loss. An antenna with perfect circular polarization ( $AR = 0$  dB) has no polarization loss. Thus, improving the reflection coefficient magnitude,  $|S_{11}|$  results in improving the total antenna efficiency,  $\eta$ , according to (1). Also, improving the AR of a circularly polarized antenna results in reducing the losses,  $L$ , and thereby enhancing both the radiation efficiency according to (2) and the total efficiency according to (1). It is shown in the parametric study, Section 2.2, that the dimensions of the antenna presented in Figure 1 can be optimized to enhance the impedance matching and AR bandwidth and, also, to enhance the radiation efficiencies expressed in (1) and (2).

The best values of these dimensional parameters are listed in Table 1. These optimum dimensions give the best performance of the proposed CP antenna regarding the circular polarization, 3 dB-AR bandwidth, impedance matching bandwidth, and radiation efficiency.

**Table 1.** Best values of the dimensional parameters of the proposed CP patch antenna.

Parameter	$L_s$	$W_S$	$L_g$	$W_g$	$L_f$	$g$	$W_f$	$s$	$s_1$	$s_2$	$g_s$
Value (mm)	40	50	15	22.7	14.8	0.2	4.2	1	1	1	0.5
Parameter	$L_1$	$L_2$	$L_3$	$L_4$	$L_5$	$W_{sp}$	$L_6$	$L_7$	$L_8$	$L_9$	
Value (mm)	6	15	20	14	7	4	12	10	5	8	

### 2.2. Parametric Study for Optimum Design of the Proposed Antenna

The design process of the proposed antenna is based on an extensive parametric study to arrive at the best values of the antenna geometrical parameters listed in Table 1. In this section, three examples of

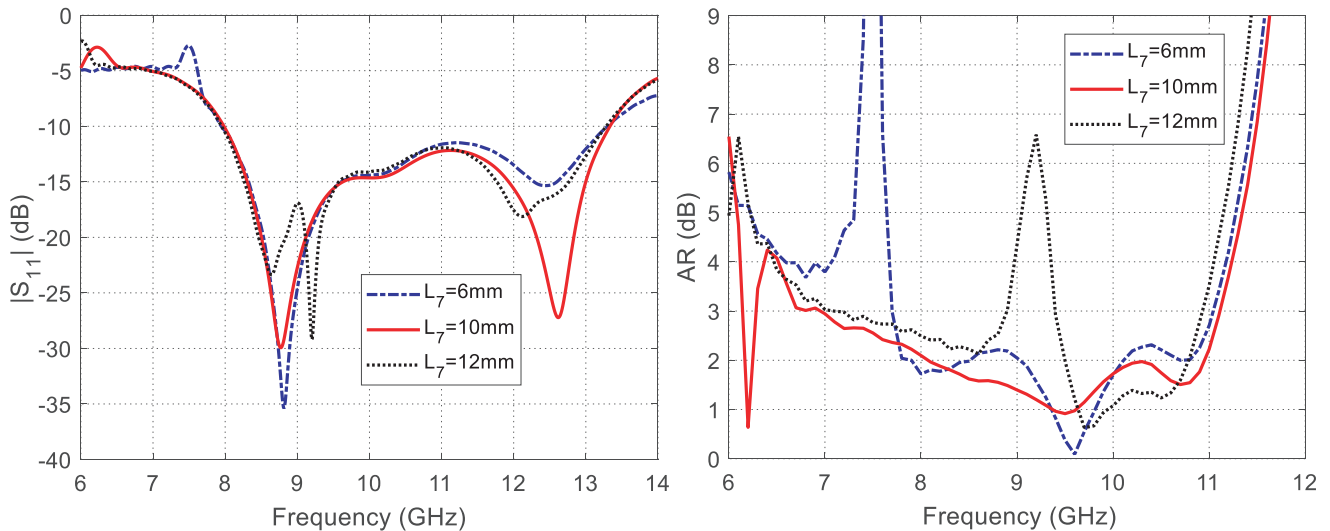


**Figure 2.** Effect of varying the horizontal length,  $L_7$ , of the corner-shaped narrow strip parasitic element, on  $|S_{11}|$  and the AR, over the frequency ranges of concern.

the parametric sweeps performed to arrive at the values of the most important dimensional parameters are presented and discussed.

To demonstrate the role of the corner-shaped narrow strip parasitic elements that are capacitively coupled to the turn-like strip radiator, the effects of changing the lengths  $L_7$  and  $L_6$  on  $|S_{11}|$  and the AR are presented in Figures 2 and 3, respectively. It is shown that the changes of both  $L_7$  and  $L_6$  do not affect the impedance matching frequency band (the band over which  $|S_{11}| < -10$  dB). However, both  $L_7$  and  $L_6$  have significant effects on the AR. It is clear that the maximum 3dB-AR is obtained when  $L_7 = 10$  mm and  $L_6 = 12$  mm.

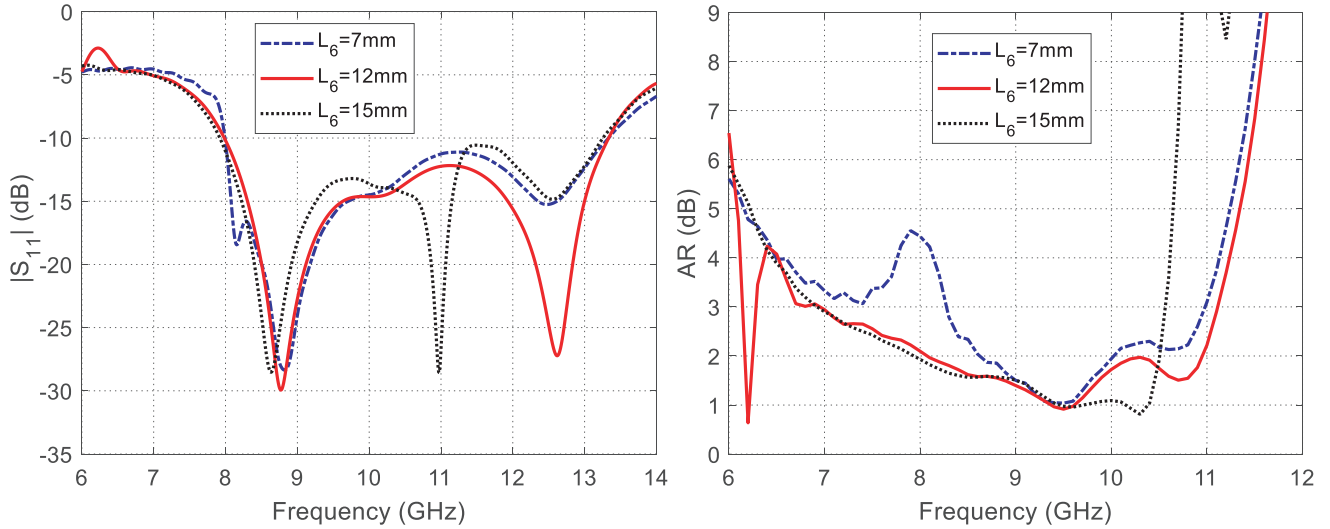


**Figure 3.** Effect of varying the vertical length  $L_6$ , on  $|S_{11}|$  and the AR, over the frequency ranges of concern.

The effects of changing the length,  $L_5$ , of the horizontal strip termination of the turn-like strip radiator on the reflection coefficient magnitude  $|S_{11}|$  and the AR are presented in Figure 4. It is shown that the reflection coefficient seems insensitive to the changes of  $L_5$ . However, the changes of this dimensional parameter significantly affect the AR over a wide range of the frequency. It is clear that setting  $L_5 = 7$  mm results in the best circular polarization and the widest 3dB-AR.

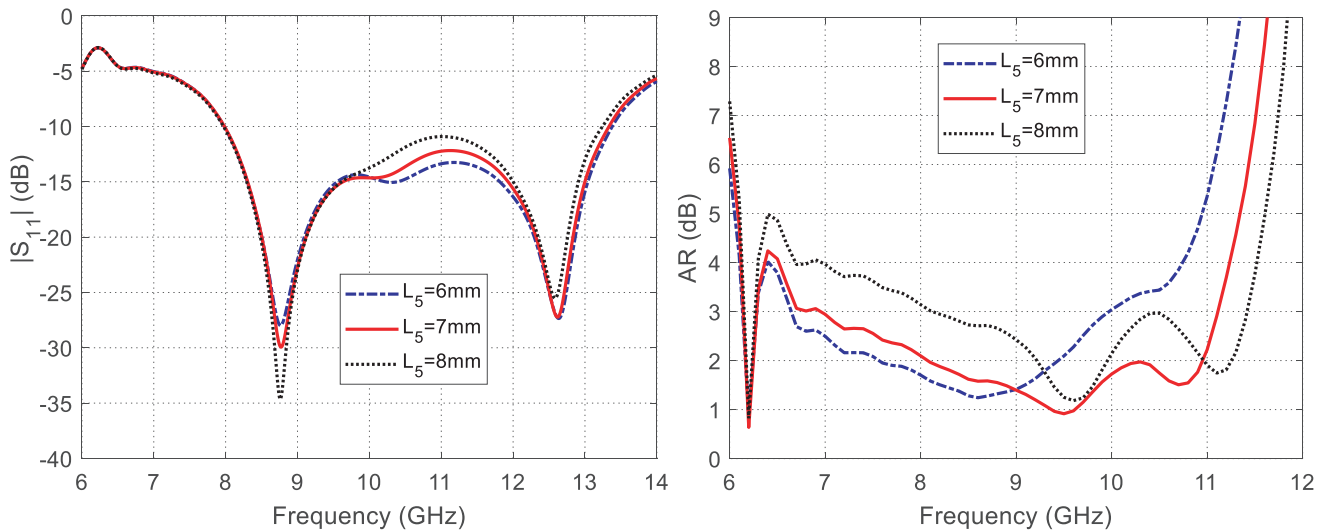


**Figure 4.** Effect of varying the length,  $L_5$ , of the horizontal termination of the turn-like strip radiator on  $|S_{11}|$  and the AR, over the frequency ranges of concern.

The effects of changing the length,  $L_9$ , of the rectangular annular slots in the sidegrounds of the CPW on the reflection coefficient magnitude  $|S_{11}|$  and the AR are presented in Figure 5. It is shown that the reflection coefficient seems insensitive to the changes of  $L_9$  also. However, the variation of this dimensional parameter significantly affects the AR over a wide range of the frequency. It is clear that setting  $L_9 = 8$  mm results in the best circular polarization and the largest 3 dB-AR bandwidth.

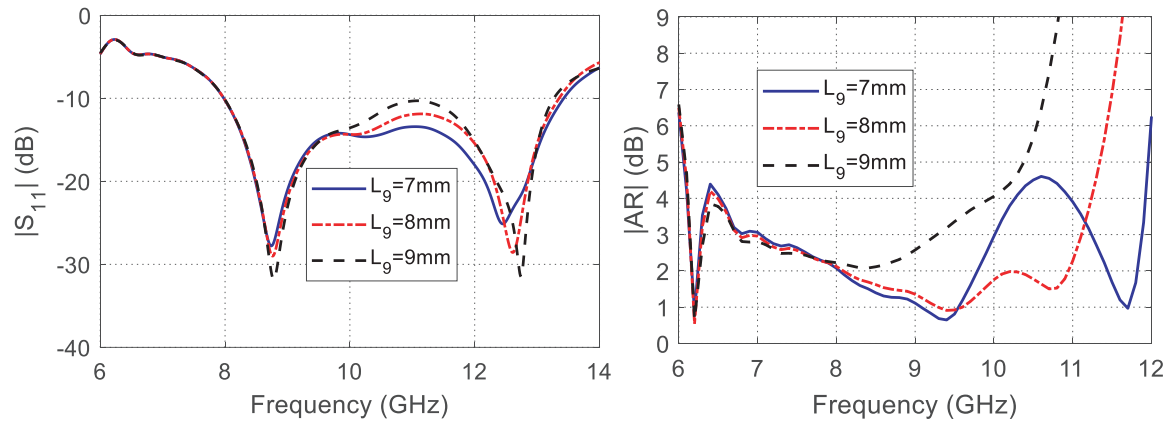


**Figure 5.** Effect of varying the length of rectangular annular slots of the CPW ground,  $L_9$ , of the turn-like strip radiator on  $|S_{11}|$  and the AR, over the frequency ranges of concern.

### 3. FABRICATION AND MEASUREMENT OF THE REFLECTION COEFFICIENT

For the purpose of experimental assessment of the proposed CP antenna, the prototype presented in Figure 6 is fabricated using lithography process and attached to a sub-miniature version A (SMA) connector for measurement. The reflection coefficient is measured using the Agilent Field fox vector network analyzer (VNA) model N9918A where the measurement setup is presented in Figure 7. The frequency response of  $|S_{11}|$  is presented in Figure 8(a) where the experimental results are compared to the simulation ones showing good agreement. It is shown that the impedance matching bandwidth is about 5.3 GHz (8–13.3 GHz) whereas the 3 dB-AR bandwidth is about 4.4 GHz (6.7–11.1 GHz) as shown in Figure 8(b). Thus, the operational bandwidth to produce good circular polarization and impedance matching at the same time is about 3.1 GHz (8–11.1 GHz).

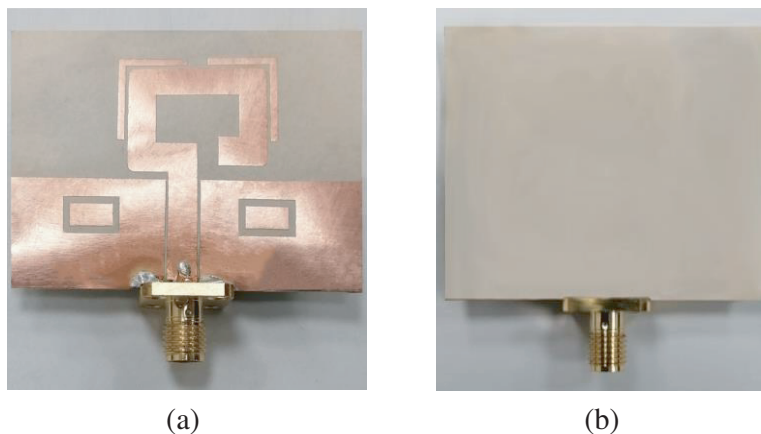


**Figure 6.** (a) Top, and (b) bottom views of the fabricated antenna mounted to the coaxial SMA connector.

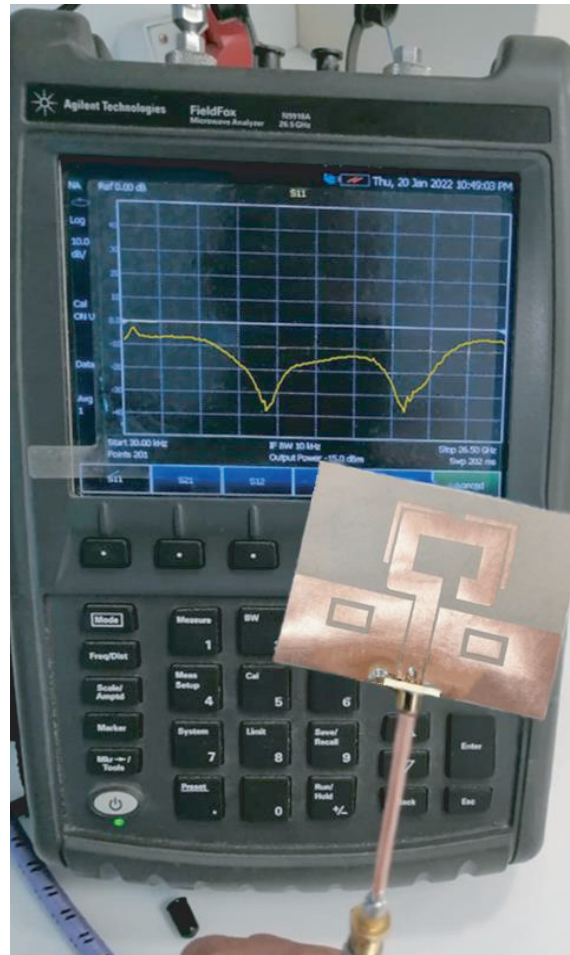


**Figure 7.** Measurement of  $S_{11}$  at the antenna port using the VNA model N9918A.

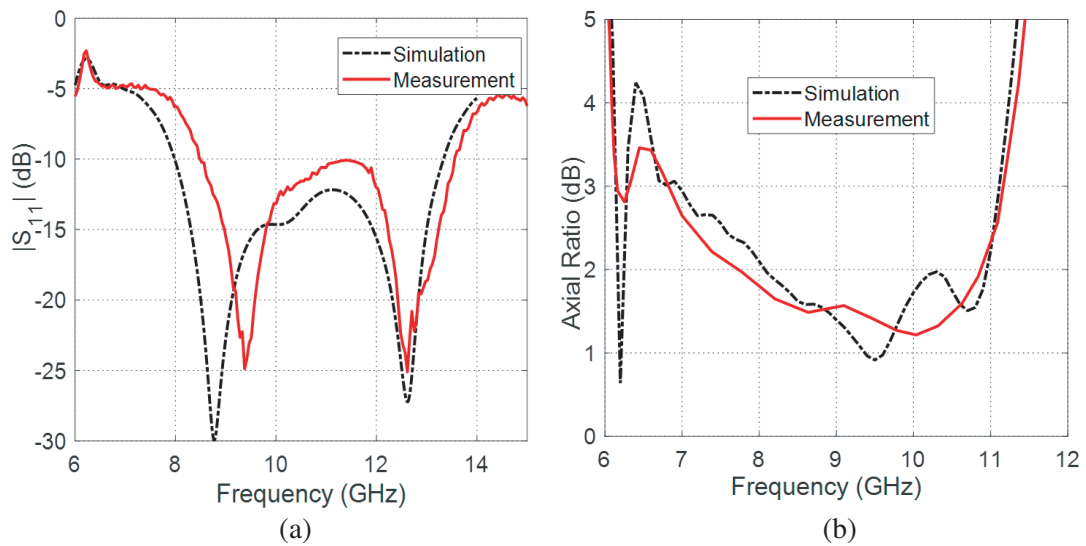


**Figure 8.** Measured and simulated frequency response of (a)  $|S_{11}|$  and (b) AR.

### 4. SURFACE CURRENT DISTRIBUTION

The characteristics of the radiated field in the far zone can be determined by the current distribution on the antenna surface. Figure 9 shows the current distribution on the conducting surface of the antenna at sequential phases  $0^\circ$ ,  $90^\circ$ ,  $180^\circ$ , and  $270^\circ$  over one cycle of the sinusoidal wave at 8.7 GHz. It is shown that, at these sequential phases, the current flows in the +ve  $y$ , +ve  $x$ , -ve  $y$ , and ve  $x$  directions, respectively. Thus, the spatial circulation (sequential directions) of the current are synchronized with

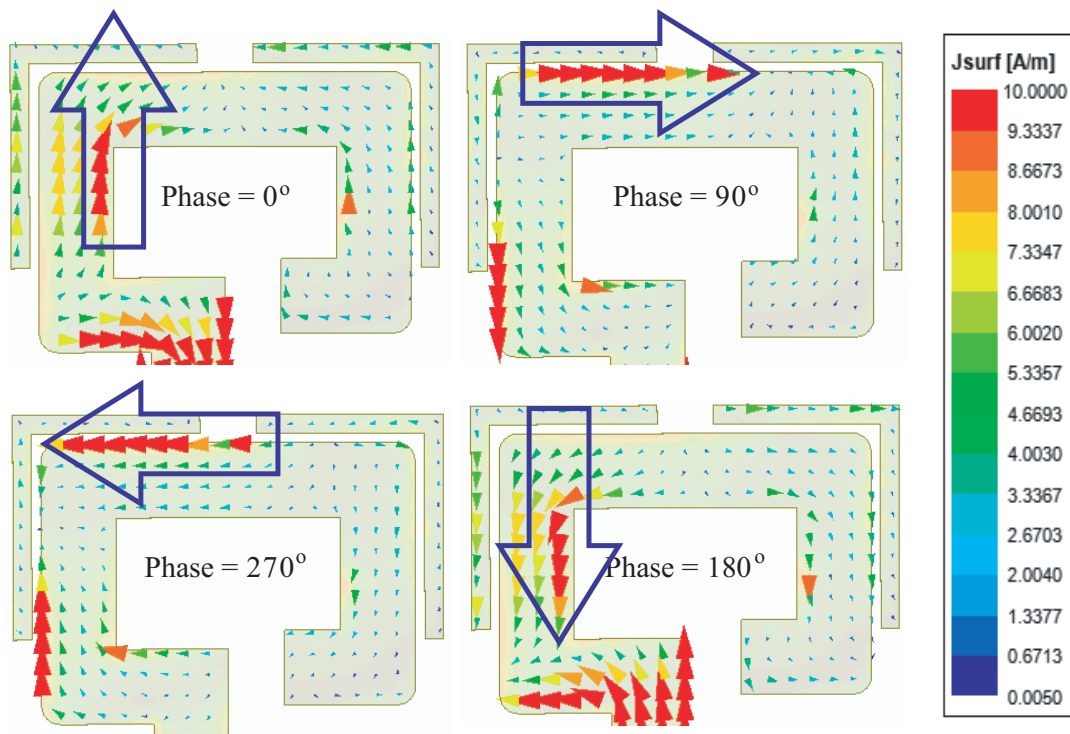


**Figure 9.** Current distribution on the proposed CP antenna surface at 8.7 GHz.

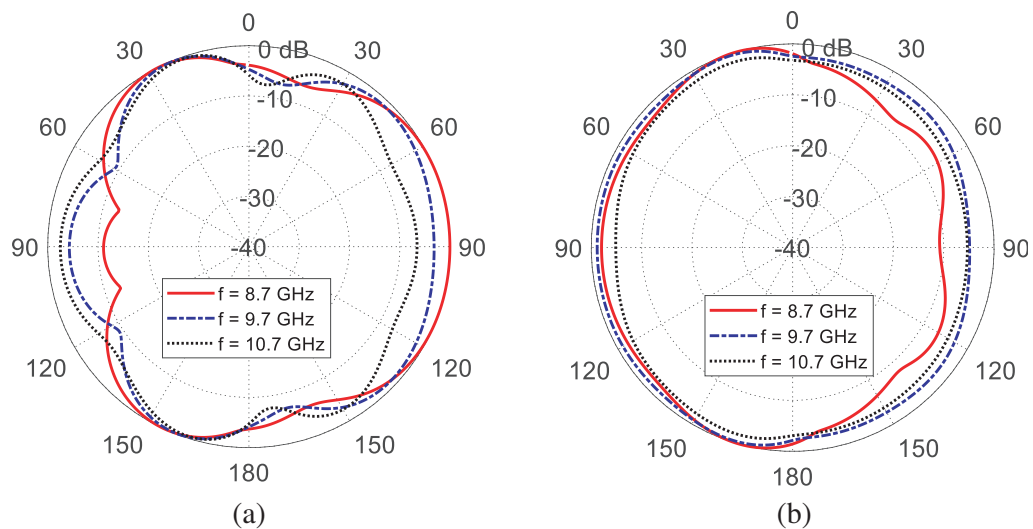


**Figure 10.** Radiation patterns of the proposed antenna in the (a) azimuth plane  $\phi = 0^\circ$  and (b) elevation plane  $\phi = 90^\circ$ , for the total field at different frequencies.

the temporal circulation (sequential phases) of the continuous wave. This indicates that the radiated field in the far zone is circularly polarized.

## 5. RADIATION PATTERNS

The far field patterns of the total radiated field at different frequencies over the operational band are numerically investigated by the CST® simulator and presented in Figure 10. The far field patterns of the total radiated field at 8.7, 9.7, and 10.7 GHz are obtained by both simulation and experimental measurements and are presented in Figures 11, 12, 13, respectively. The far field patterns of the cross polarized fields (RHCP and LHCP) are presented in Figure 14. It is shown that the radiated field is dominated by left hand circular polarization (LHCP) component in the positive  $z$ -direction and right hand circular polarization (RHCP) component in the negative  $z$ -direction. If the turn-like strip radiator

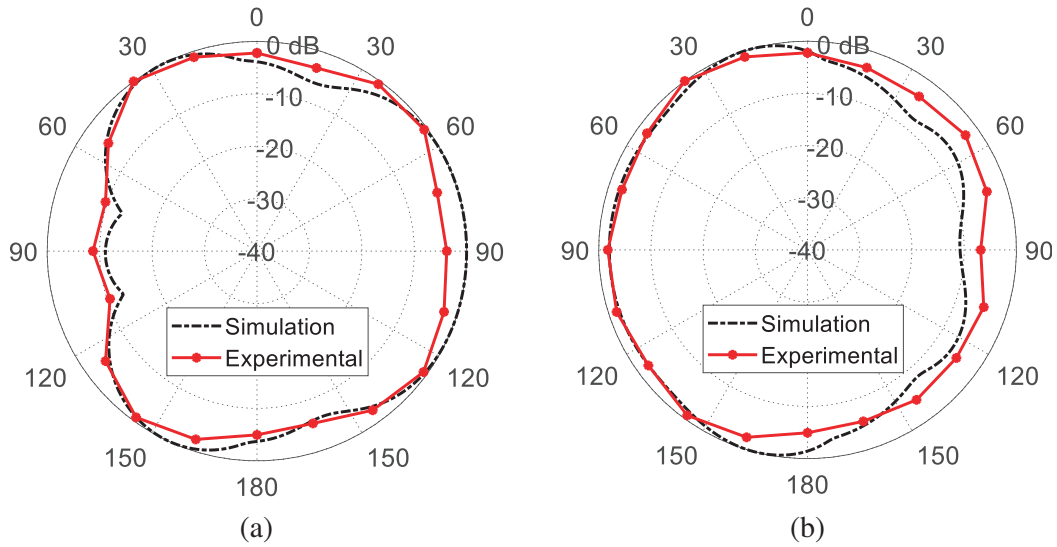


**Figure 11.** Measured radiation patterns of the proposed antenna in the (a) azimuth plane  $\phi = 0^\circ$  and (b) elevation plane  $\phi = 90^\circ$  for the total field at 8.7 GHz.

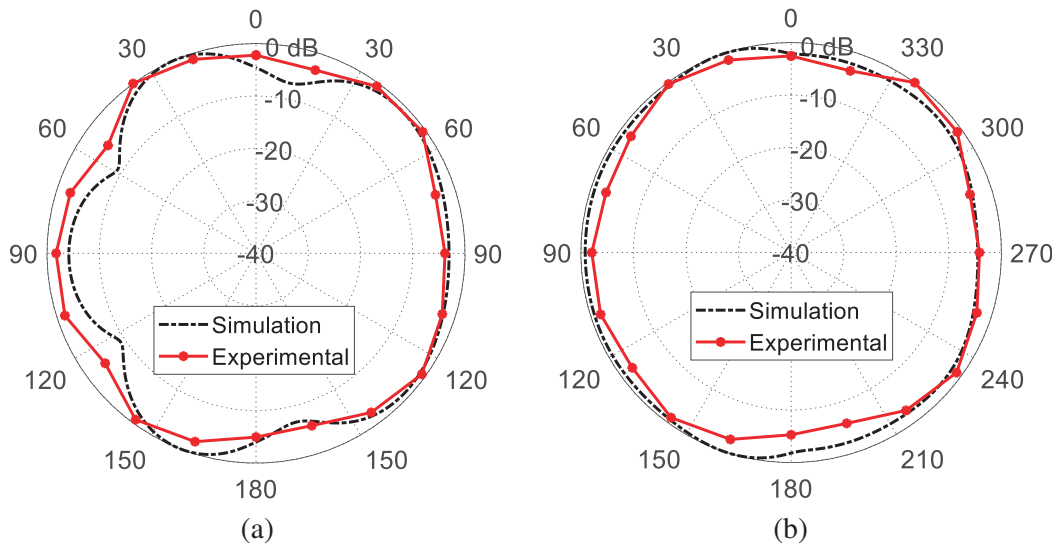


**Figure 12.** Measured radiation patterns of the proposed antenna in the (a) azimuth plane  $\phi = 0^\circ$  and (b) elevation plane  $\phi = 90^\circ$  for the total field at 9.7 GHz.

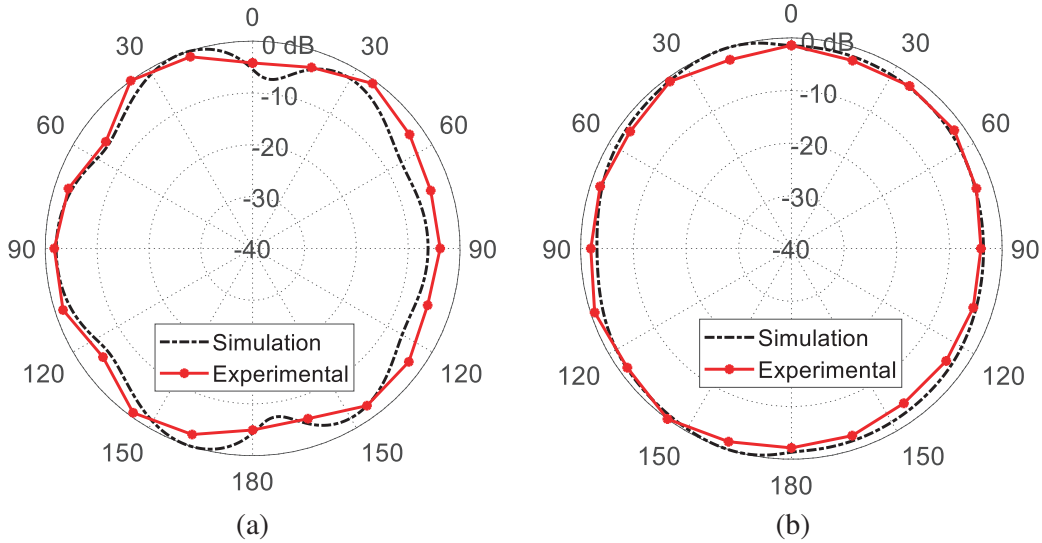


**Figure 13.** Measured radiation patterns of the proposed antenna in the (a) azimuth plane  $\phi = 0^\circ$  and (b) elevation plane  $\phi = 90^\circ$  for the total field at 10.7 GHz.

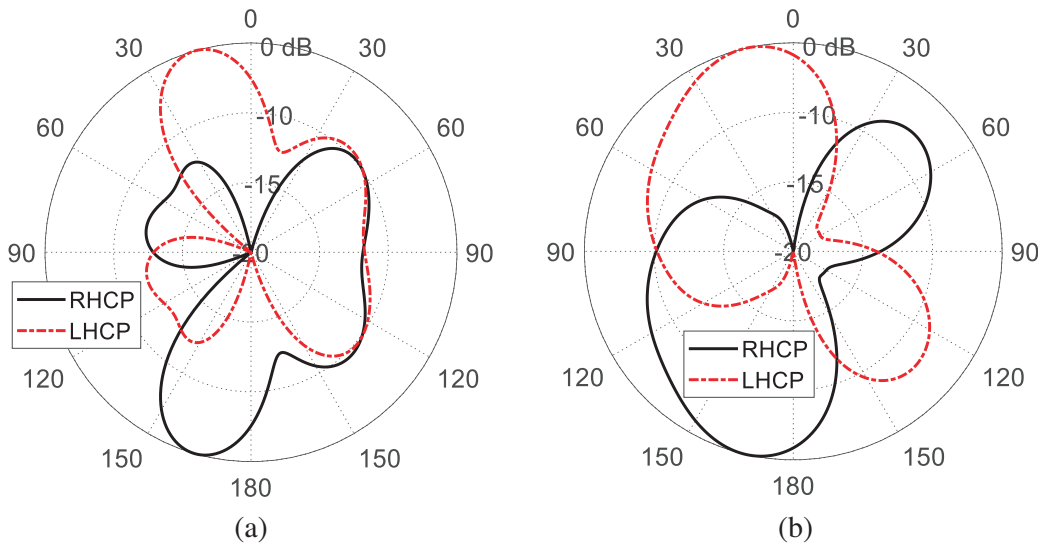


**Figure 14.** RHCP and LHCP radiation patterns of the proposed antenna in the (a) azimuth plane  $\phi = 0^\circ$  and (b) elevation plane  $\phi = 90^\circ$ , at 9.7 GHz.

were mirrored, the radiated field would be dominated by RHCP component in the positive  $z$ -direction and LHCP component in the negative  $z$ -direction keeping the same antenna performance regarding the impedance matching, 3 dB-AR bandwidth, and antenna efficiency.

### 6. GAIN AND RADIATION EFFICIENCY

The maximum total gain and radiation efficiency of the proposed CP antenna are presented in Figures 15(a) and 15(b) over a wide frequency range. The simulation results are compared to the experimental measurements showing good agreement. As shown in Figure 15(a), the maximum gain of the total radiated field varies between 4.4 and 5 dBi over the frequency band of concern (8–11.1 GHz). On the other hand, the antenna exhibits very high radiation efficiency that is greater than 99% over the same frequency band.

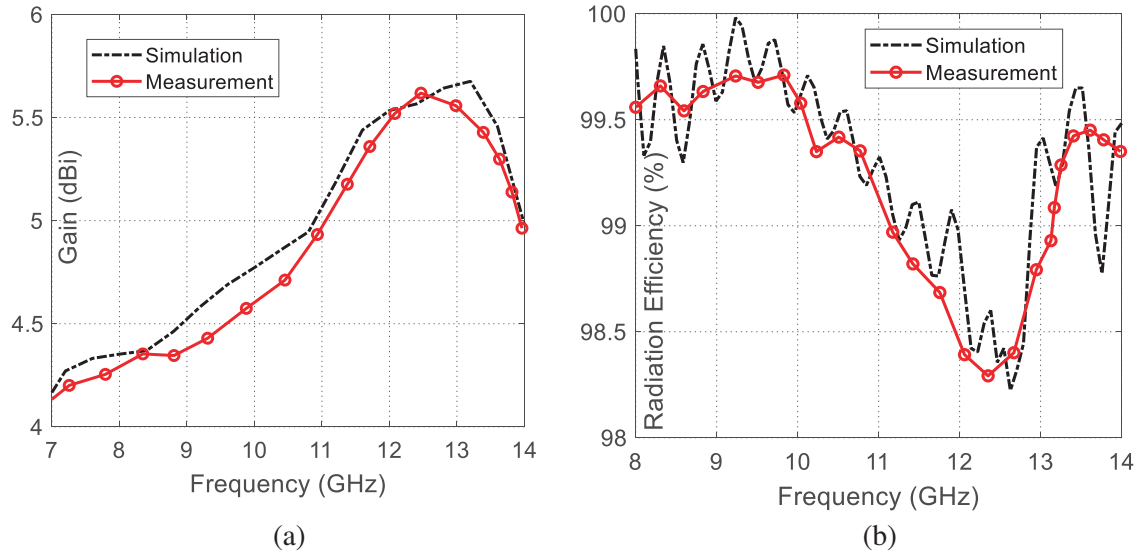


**Figure 15.** Frequency dependence of the (a) gain, and (b) radiation efficiency, over the operational frequency band for the proposed antenna.

## 7. COMPARISON WITH PUBLISHED WORK

To present the achievements of the present work in the context of the recent research work of the same interests, a brief summary of comparisons is listed in Table 2. The comparative summary includes the antenna dimensions, the impedance matching, the operational frequency bandwidths, the maximum gain over the operational frequency band, and the average radiation efficiency.

**Table 2.** List of performance measures of the proposed antenna in comparison to other published planar wideband antenna designs.

Work	Dimensions (mm <sup>3</sup> )	Operating Frequency Bands (GHz) / (%)	Axial ratio Bandwidth (%)	Average Gain (dBi)	Average Radiation Efficiency (%)
[2]	28 × 23.9 × 1.6	3.64–15.30 (123%)	3.85–10.52 GHz (93%)	3.3 dBi	94%
[4]	20 × 20 × 1.5	4.0–15 (115.78%)	6.6–11.82 GHz (56.67%)	5.5	NA
[5]	48 × 29.5 × 1.6	3.07 to 3.81 4.64 to 6.21 (21.5%, 29.4%)	670 MHz, 590 MHz	NA	NA
[10]	60 × 60 × 0.8	2.04–7.95 (118.2%)	3.6–6.84 GHz (62%)	2.7 dBi to 4.32	92% to 95.4%
[11]	50 × 50 × 1	1.75–4.5 (88%)	2.3–4.5 GHz (62%)	2.3 dBi	90%
[Present]	40 × 50 × 0.13	8–13.3 (50%)	8–11.1 GHz (32%)	5.7	99.2%

## 8. CONCLUSION

A wide band CP planar antenna of high radiation efficiency has been proposed and investigated by simulation and experimental measurements. The antenna is fed through CPW region whose ground structure is defected by etching two rectangular annular slots. Both the corner-shaped parasitic elements and the rectangular annular slots of the CPW ground plane help to increase the impedance matching and 3 dB axial ratio (AR) bandwidths, and to enhance the antenna efficiency. Both the simulation results and experimental measurements show that the impedance matching bandwidth is about 5.3 GHz (8–13.3 GHz); the 3 dB AR bandwidth is about 3.1 GHz (8–11.1 GHz); the maximum gain ranges from 4.5 to 5.5 dBi; and the radiation efficiency is greater than 98% over the operational frequency band.

## REFERENCES

1. Lin, W. P. and C. H. Huang, "Coplanar waveguide-fed rectangular antenna with an inverted-L stub for ultrawideband communications," *IEEE Antennas and Wireless Propagation Letters*, Vol. 8, 228–231, 2009.
2. Mondal, K., "Axial Ratio (AR) and Impedance Bandwidth (IBW) enhancement of Circular Polarized (CP) monopole antenna," *AEU — International Journal of Electronics and Communications*, Vol. 134, 153649, 2021.
3. Chen, B. and F. S. Zhang, "Dual-band CPW-fed circularly polarized slot antenna with improved ground plane structure," *Progress In Electromagnetics Research Letters*, Vol. 46, 31–36, 2014.
4. Jaiverdhan, M. M. S., R. P. Yadav, and R. Dhara, "Characteristic mode analysis and design of broadband circularly polarized CPW-fed compact printed square slot antenna," *Progress In Electromagnetics Research M*, Vol. 94, 105–118, 2020.
5. Radhakrishnan, R. and S. Gupta, "Axial ratio tuned circularly polarized slot-loaded antenna for S-band and C-band applications," *Progress In Electromagnetics Research C*, Vol. 113, 239–249, 2021.
6. Bao, X. L. and M. J. Ammann, "Dual-frequency dual-sense circularly polarized slot antenna fed by microstrip line," *IEEE Trans. Antennas Propag.*, Vol. 56, No. 3, 645–649, 2008.
7. Chen, C. and E. K. N. Yung, "Dual-band dual-sense circularly-polarized CPW-fed slot antenna with two spiral slots loaded," *IEEE Trans. Antennas Propag.*, Vol. 57, No. 6, 1829–1833, 2009.
8. Chen, Y. Y., Y. C. Jiao, G. Zhao, F. Zhang, Z. L. Liao, and Y. Tian, "Dual-band dual-sense circularly polarized slot antenna with a C-shaped grounded strip," *IEEE Antennas and Wireless Propagation Letters*, Vol. 10, 915–918, 2011.
9. Saini, R. K., S. Dwari, and M. K. Mandal, "CPW-fed dual-band dual-sense circularly polarized monopole antenna," *IEEE Antennas and Wireless Propagation Letters*, Vol. 16, 2497, 2017.
10. Banerjee, U., A. Karmakar, A. Saha, and P. Chakraborty, "A CPW-fed compact monopole antenna with defected ground structure and modified parasitic hilbert strip having wideband circular polarization," *Int. J. Electron. Commun.*, Vol. 110, 152831, 2019.
11. Ding, K., C. Gao, C. Y. Wu, D. Qu, and B. Zhang, "A broadband circularly polarized printed monopole antenna with parasitic strips," *IEEE Antennas and Wireless Propagation Letters*, Vol. 16, 2509, 2017.
12. Ding, K., Y. X. Guo, and C. Gao, "CPW-fed wideband circularly polarized printed monopole antenna with open loop and asymmetric ground plane," *IEEE Antennas and Wireless Propagation Letters*, Vol. 16, 833–836, 2017.